

Quantifying tau PET imaging reliably in the presence of off-target binding

MIR Mallinckrodt Institute
of Radiology

KnightADRC WASHINGTON UNIVERSITY ST. LOUIS
Alzheimer's Disease Research Center

Charles D. Chen^a, Brian A. Gordon^{a,b}, Austin McCullough^a, Aiad Zaza^a, Christopher Mejias^a, Aylin Dincer^a, Shaney Flores^a, Sarah Keefe^a, Angela Paulick^a, Kelley Jackson^a, Deborah Koudelis^a, Yi Su^c, John C. Morris^{b,d}, Tammie L.S. Benzinger^{a,b}
^aMallinckrodt Institute of Radiology, ^bKnight Alzheimer's Disease Research Center, and ^dDepartment of Neurology,
Washington University in St. Louis, St. Louis, MO, USA, and ^cBanner Alzheimer's Institute, Banner Health, Phoenix, AZ, USA

Banner
Alzheimer's Institute

Introduction

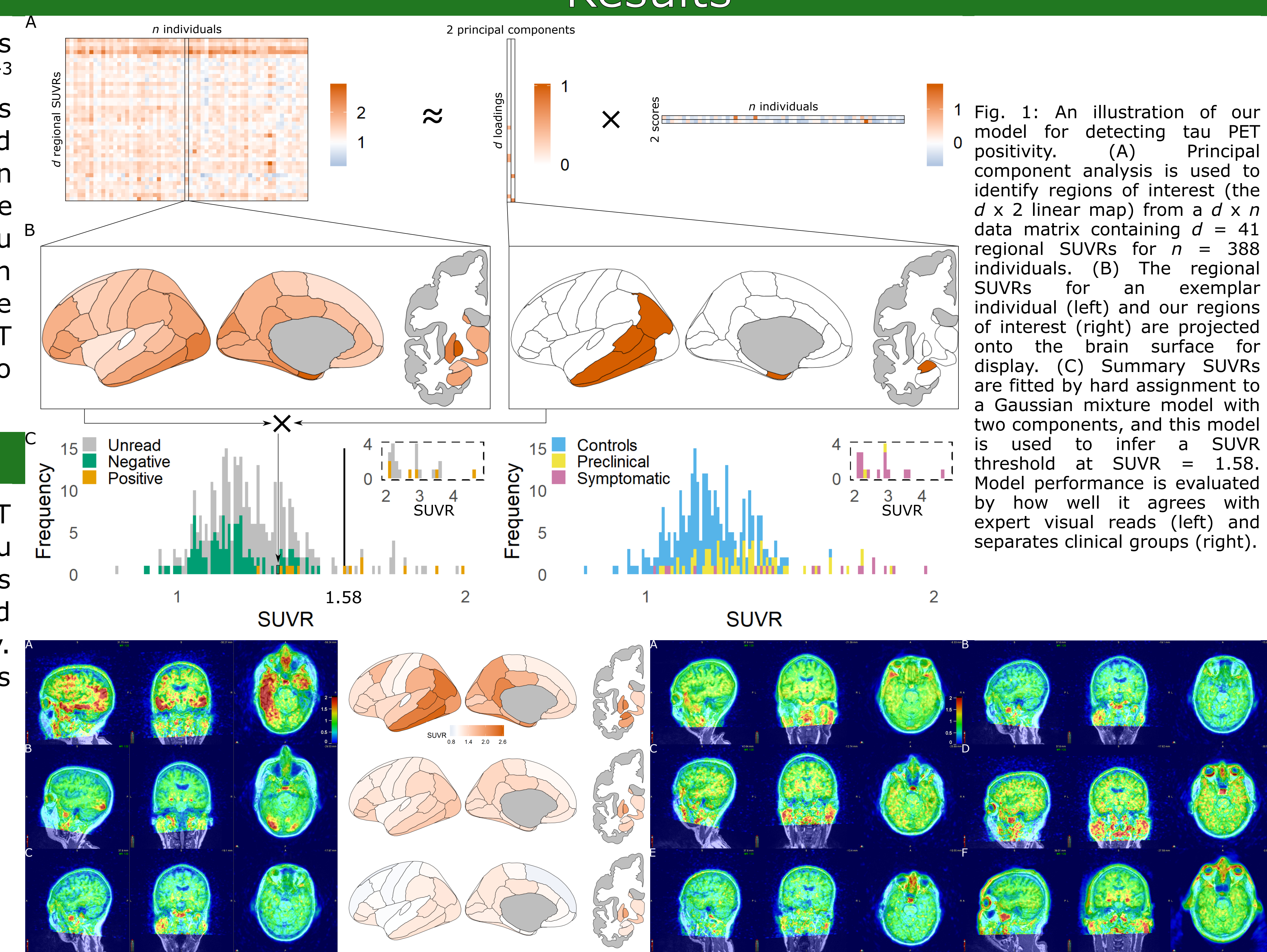
Tau PET imaging is a powerful tool for studying the *in vivo* pattern of neurofibrillary tangles across the brain, and has rapidly become a crucial biomarker for Alzheimer's disease.¹⁻³ While elevated tau tracer uptake is a consistent finding in individuals with Alzheimer's disease, there is a lack of consensus on which regions of interest and SUVR threshold should be used for detecting images positive for tau pathology^{4,5}. Further difficulties lie in confounding tracer signals from age-related effects⁶⁻⁸, off-target binding⁹⁻¹², and the heterogeneity of Alzheimer's disease progression¹³⁻¹⁵. Current approaches for detecting tau PET positivity require strong *a priori* assumptions about the frequencies of tau positivity with respect to amyloid positivity and cognitive impairment in order to mitigate these difficulties^{4,16,17}. Such assumptions could raise new complications when translating tau PET imaging results into future clinical use in situations where these frequency priors are no longer reasonable assumptions.

Methods

To address such complications, we propose an unsupervised model for detecting tau PET positivity with minimal assumptions. Our model is solely informed by ¹⁸F-floratacupir tau PET imaging data from a cohort spanning the spectrum from normal aging to Alzheimer's disease ($n = 388$). The model relies on two steps: first, principal component analysis is used to identify regions of interest that account for variability in tracer uptake due to pathology. Second, a Gaussian mixture model is used to infer a SUVR threshold for tracer uptake across these regions of interest.

	CDR = 0	CDR > 0
Number	340	58
Age, years (SD)	69.3 (8.42)	75.3 (6.36)
Female (%)	195 (57.4%)	29 (50.0%)
Education, years (SD)	16.3 (2.30)	15.4 (2.85)
MMSE, score (SD)	29.2 (1.12)	25.9 (3.65)
APOE ε4 (24/34/44)	113 (9/94/10)	32 (0/26/6)

Table 1: Cohort demographics.
* APOE ε4 was only available for 337/340 of the CDR = 0 cohort and 53/58 of the CDR > 0 cohort.



Discussion

We evaluated model performance with expert visual reads (error rate = 4.58%, $n = 131$), clinical groups (controls vs preclinical Alzheimer's disease, Cliff's $d = 0.49$, preclinical versus symptomatic, Cliff's $d = 0.63$, $n = 330$), and current approaches for detecting tau PET positivity (error rates = 5.34% to 43.5%). Our results suggest our unsupervised model improves upon the accuracy of current approaches while avoiding biases from clinical diagnoses. Our model identifies the amygdala, banks of the superior temporal sulcus, and entorhinal, inferior parietal, inferior temporal, and middle temporal cortices as regions of interest, and infers a SUVR threshold of $SUVR = 1.58$.

References

- ¹Jack et al. (2016), ²Saint-Aubert et al. (2017), ³Leuzy et al. (2019), ⁴Jack et al. (2017), ⁵Maass et al. (2017), ⁶Crary et al. (2014), ⁷Choi et al. (2018), ⁸Lowe et al. (2018a), ⁹Marquie et al. (2015), ¹⁰Johnson et al. (2016), ¹¹Lowe et al. (2016), ¹²Lemoine et al. (2018b), ¹³Jack et al. (2018), ¹⁴Lowe et al. (2018), ¹⁵Charil et al. (2019), ¹⁶Mishra et al. (2017), ¹⁷Ossenkoppel et al. (2018).

	Our model	Ossenkoppel et al. (2018)		Jack et al. (2017)		Mishra et al. (2017)
		Mean + 2 SDs	Youden Index	Specificity	Sensitivity	
SUVR threshold	1.58	1.68	1.27	1.43	1.21	1.21
True positive	13	9	19	15	19	19
False positive	0	0	30	3	57	30
False negative	6	10	0	4	0	0
True negative	112	112	82	109	55	82
Error rate	4.58%	7.63%	22.9%	5.34%	43.5%	22.9%
Controls vs preclinical	0.49	0.44	0.44	0.44	0.44	0.47
Preclinical vs Symptomatic	0.63	0.59	0.59	0.60	0.60	0.64

Fig. 2 (left): Exemplar SUVbw (left) and group-averaged images (right) of (A) true positives, (B) false negatives, and (C) true negatives as classified by our model and evaluated by expert visual reads.

Fig. 3 (right): SUVbw images of six of the 23 false positives in common among the "Youden Index", "sensitivity", and "SKM clustering" approaches. (A-F) No appreciable uptake clearly reflecting tau pathology.

Table 2: Approaches for detecting tau PET positivity.

* Error rate = $(FP+FN)/(TP+FP+FN+TN)$.

** Group differences are reported in Cliff's d .

Acknowledgements

We acknowledge support from the Knight Alzheimer's Disease Research Center (P50AG005681, P01AG026276, and P01AG003991) and the Neuroimaging Informatics and Analysis Center (P30NS098577). CDC (DGE-1745038). BAG (K01AG053474, U19AG032438)